Online Research @ Cardiff

This is an Open Access document downloaded from ORCA, Cardiff University's institutional repository: http://orca.cf.ac.uk/87889/

This is the author's version of a work that was submitted to / accepted for publication.

Citation for final published version:

Stacey, Oliver J., Ward, Benjamin David, Amoroso, Angelo JAmes and Pope, Simon J. A. 2016. Near-IR luminescent lanthanide complexes with 1,8-diaminoanthraquinone-based chromophoric ligands. Dalton Transactions 45 (15) , pp. 6674-6681. 10.1039/C5DT04351D file

Publishers page: http://dx.doi.org/10.1039/C5DT04351D <http://dx.doi.org/10.1039/C5DT04351D>

Please note:
Changes made as a result of publishing processes such as copy-editing, formatting and page numbers may not be reflected in this version. For the definitive version of this publication, please refer to the published source. You are advised to consult the publisher's version if you wish to cite this paper.

This version is being made available in accordance with publisher policies. See http://orca.cf.ac.uk/policies.html for usage policies. Copyright and moral rights for publications made available in ORCA are retained by the copyright holders.

information services
gwasanaethau gwybodaeth

Near-IR luminescent lanthanide complexes with 1,8-diaminoanthraquinone-based chromophoric ligands†

Oliver J. Stacey, Benjamin D. Ward, Angelo J. Amoroso and Simon J. A. Pope*

Three new chromophoric anthraquinone-based multidentate ligands have been synthesised in a step-wise manner from 1,8-dichloroanthraquinone. The ligands each comprise two dipicolyl amine units and react with trivalent lanthanide ions to form monometallic complexes of the form [Ln(L)](OTf)$_3$ as indicated by MS studies and elemental analyses. Supporting DFT studies show that the monometallic species are highly favoured (>1000 kJ mol^{-1}) over the formation of a 2 : 2 dimetallic congener. Both ligands and complexes absorb light efficiently ($\varepsilon \sim 10^4$ M^{-1} cm^{-1}) in the visible part of the spectrum, with λ_{abs} ca. 535–550 nm through an intramolecular charge transfer (ICT) transition localised on the substituted anthraquinone unit. In all cases the complexes show a fluorescence band at ca. 675 nm due to the ICT emitting state. The corresponding Nd(III), Yb(III) and Er(III) complexes also reveal sensitised near-IR emission characteristic of each ion following excitation of the ICT visible absorption band at 535 nm.

Introduction

The use of substituted anthraquinone derivatives as ligands, or as a component of ligands, for metal ions is well known and has been recently detailed.[1] The commercial availability of a number of substituted anthraquinone species, together with their rich electronic and redox properties, has allowed wide-ranging variants to be investigated. Anthraquinones have been historically used as dyes and pigments,[2] but are also well known in nature (occuring in both plant and insect life) pro-viding stimulation for biological and medicinal products[3] based on the anthraquinone core (for example, Fig. 1).

The electronic properties of substituted anthraquinones have been investigated in detail.[4] Unsubstituted anthra-quinone possesses dominant $^1\pi$–π^* transitions between 220–350 nm with a much weaker ^{1}n–π^* transition, due to the presence of the carbonyl groups, around 400 nm.[5] The addition of substitutents to the anthraquinone core pro-foundly influences these optical properties. Of most interest are the influence of electron donating groups, such as amine, hydroxyl, alkoxy, which impart varying degrees of intra-molecular charge transfer (ICT) character to π–π^* transitions; for example, 1-aminoanthraquinone has a lowest energy absorbtion at ca. 480 nm.[5,6] Multiple amino-substituents can bathochromically shift the absorption wavelength; in 1,4-versus 1,5-substituted species, computational studies have suggested that the varied distribution of the HOMO dominates the modulation of the HOMO–LUMO energy gap.[7]

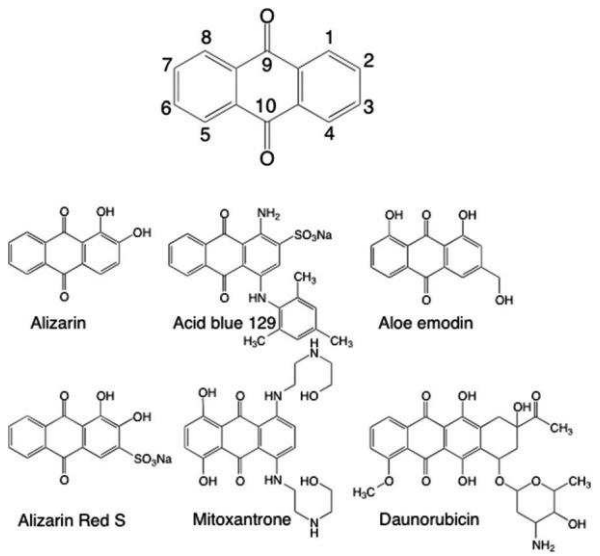

Fig. 1 Anthraquinone (top) and a selection of derivatives for use as dyes (Alizarin, Alizarin Red S, Acid blue 129) and medicinal agents (Aloe emodin, Mitoxantrone, Daunorubicin).

The coordination chemistry of a small number of both acyclic and macrocyclic ligands based upon 1,8-disubstituted

School of Chemistry, Main Building; Cardiff University, Cardiff CF10 3AT, UK. E-mail: popesj@cardiff.ac.uk; Fax: +44(0) 029-20874030; Tel: +44(0) 029-20879316

anthraquinones have been reported. For example, Pd(II) can form square planar complexes with 1,8-diamino-derived ligands including coordinative participation of the quinone.[8] The rich optical characteristics of anthraquinone species has encouraged significant interest in their application as chromo-genic sensors.[9] Ligands possessing a variety of receptor environments for binding metal ions have been developed, including a colourimetric response to Cu(II) with strong perturbation of the ICT bands of the anthraquinone chromo-phore.[10,11] Very recent work by Sykes and Mariappan has described sulfur, selenium and tellurium analogues of 1,8-anthraquinone-18-crown-5 for the targeted binding of Pb(II).[12]

Our own studies have investigated the development of Au(I) complexes of alkynylalkoxy derivatives of anthraquinone for use as fluorescent cell imaging agents.[13] Alkynyl groups can also be directly attached to the anthraquinone core and explored in Pt(II) coordination chemistry.[14]

We have previously shown that anthraquinone-based chromophores can be covalently linked to DO3A-like binding sites for trivalent lanthanide ions allowing both monometallic[15] and dimetallic variants to be synthesised, the latter investi-gated for DNA binding interactions and the resultant modu-lation of Gd(III)-enhanced water relaxivity properties.[16]

This paper focuses on the stepwise synthesis of three new acyclic polydentate ligands that are based upon a 1,8-diamino-substituted anthraquinone core. The aim of the work was to explore the use of these visible light absorbing antennae as sensitizing moieties for near infrared (near-IR) emitting Ln(III). The synthesis and characterisation of the new compounds are discussed together with the time-resolved luminescence pro-perties of the complexes.

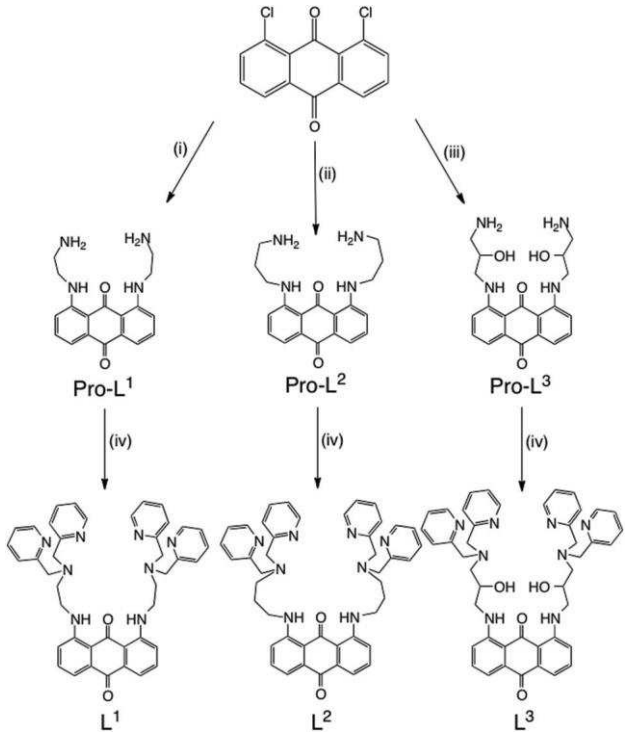

Scheme 1 The reaction pathways to the ligands (i) DMSO, excess 1,2-diaminoethane; (ii) DMSO, excess 1,3-diaminopropane; (iii) DMSO, excess 1,3-diamino-2-propanol; (iv) 1,2-DCE, 2-pyridinecarboxaldehyde, $Na(OAc)_3BH$.

Results and discussion

Synthesis and characterisation of the ligands and complexes

The new chromophoric ligands were synthesised (Scheme 1) from commercially available 1,8-dichloroanthraquinone; reac-tion with an excess of 1,2-diaminoethane, 1,3-diaminopropane or 1,3-diamino-2-propanol yielded the disubstituted anthra-quinone pro-ligand intermediates, Pro-$L^{1–3}$. These compounds were isolated as highly coloured solids: the reaction was con-veniently indicated by the progressive colour changes of the reaction mixture whereby transformation from yellow to red indicated formation of the monosubstituted intermediate, and a further change to deep purple was indicative of the 1,8-disub-stituted target (see ESI†). Of course, such observable changes render the reactions highly amenable to thin layer chromato-graphy, allowing convenient in situ monitoring of the reaction progress. Subsequent treatment of the pro-ligands with four equivalents of 2-pyridinecarboxaldehyde in the presence of $NaBH(OAc)_3$ yielded the three multidentate ligands, $L^{1–3}$, via a reductive amination procedure (Scheme 1). The corresponding lanthanide complexes (Ln-$L^{1–3}$) were obtained as deep purple coloured solids through treatment of the ligands with $Ln(OTf)_3$.

The three ligands, and their precursors, possessed good solubility in a range of common organic solvents and were characterised using a range of spectroscopic and analytical techniques. Of particular note in the ^1H NMR spectra of the species were the presence of NH resonances (as broadened tri-plets) around δ_H 9.75 ppm, which indicated the formation of the characteristic amino-substituted anthraquinone moieties. This particular resonance proved to be a convenient diagnostic signal for diff erentiating between the desired disubstituted species and any monosubstituted impurities. IR spectroscopy clearly confirmed the presence of the NH groups (~3300 cm^{-1}) and dicarbonyl quinone unit with ν(CvO) at ca. 1600 cm^{-1}. HR mass spectrometry confirmed the proposed formulations for the ligands in each case.

The paramagnetic Ln(III) complexes were also characterised using MALDI mass spectrometry which revealed the character-istic isotoptic distribution for a monometallic complex in each case (see ESI†), with no evidence for dimetallic species. The stoichiometry of a selection of the complexes was quantitat-ively confirmed using elemental analyses, suggesting a 1 : 1 (Ln : L) ratio. It should be noted that despite the identical reac-tion conditions and ligand batches used for the synthesis of the diff erent Ln(III) complexes we were unable to obtain, despite repeated attempts, representative elemental analyses for some of the complexes (notably Gd and Yb complexes), which revealed incomplete combustion as indicated by low C, H and N values, which has been noted before for some

lanthanide complexes.[17] The CHN elemental analyses obtained for the complexes of L^3 show that the complexes exist as the trication and therefore the putative alcohol donors are not deprotonated.

Computational modelling studies

Whilst the structures of the complexes $[Ln(L^n)]X_3$ are postu-lated as 1 : 1 complexes, it is theoretically possible that the complexes could exist as 2 : 2 dimeric species (with a resultant 6+ charge), with the formulation $[Ln_2(L^n)_2]X_6$; such species are of course compatible with the obtained CHN elemental analyses. In this context, HXTA (N,N-(2-hydroxy-5-methyl-1,3-xylylene)bis-(N-(carboxymethyl)glycine)) derived ligands are known to form $Na_4[Ln(HXTA)]_2$ dimetallic species with lanthanide ions (with a resultant 4− charge).[18]

DFT models were therefore employed to probe the likely structures of each of the ligands coordinated to either Y or La (thus giving two examples across an ionic radii range). In addition to calculating the structures of $[Ln(L^n)]^{3+}$, two hypothetical dimeric structures $[Ln_2(L^1)_2]^{6+}$, for Ln = Y and La were also investigated. The calculated structure of $[La(L^1)]^{3+}$ is shown in Fig. 2. Whilst the calculations do not account for explicit solvent interactions for such highly charged species, the calculations nevertheless give overwhelming support for the complexes existing in a monomeric state. An analysis of the calculated free energies for the monomer → dimer trans-formations give G = 1197 kJ mol^{-1} and 1075 kJ mol^{-1} for Y and La respectively. Whilst it is inappropriate to ascribe chemi-cal accuracy to these values, we infer that the formation of dimeric complexes is highly unlikely for this class of ligands.

For the complexes with L^1 and L^2, the metal ions are 8-coor-dinate, whilst those with L^3 are calculated to be 10-coordinate. In each of the structures, the Ln(III) ion is completely encapsu-lated by the ligand, with an interaction between the "inside" carbonyl and the metal ion inferred by $d_{Ln–O}$ = 2.249 Å ($[Y(L^1)]^{3+}$), 2.269 Å ($[Y(L^2)]^{3+}$), 2.347 ($[Y(L^3)]^{3+}$), 2.349 Å ($[La(L^1)]^{3+}$), 2.434 Å ($[La(L^2)]^{3+}$), 2.457 ($[La(L^3)]^{3+}$), which are well within the sum of the covalent radii ($\sum\{r_{cov}(Y) + r_{cov}(O)\}$ = 2.56 Å; $\sum\{r_{cov}(La) + r_{cov}(O)\}$ = 2.73 Å).[19] In each structure, one of the secondary amine nitrogens coordinates to the metal ion, whilst the non-coordinating amine internally hydrogen bonds with the coordinating carbonyl group.

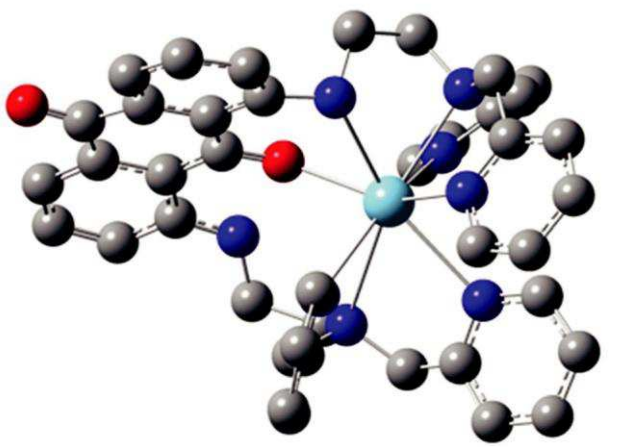

Fig. 2 The calculated structure of $[La(L^1)]^{3+}$. Hydrogen atoms are omitted for clarity.

For the complexes of L^3, two viable conformations were evident from the calculations; those with one- and two hydroxyl groups coordinated to the metal ion. Calculations of the lanthanum congener suggest that the isomer with two co-ordinated hydroxyl groups is the more stable, by 73 kJ mol^{-1}.

Electronic properties: UV-vis and luminescence data

The UV-vis absorption spectra of the free ligands were obtained on acetonitrile solutions, revealing absorbing bands throughout the visible and UV regions. The anthraquinone π–π* transitions contribute between 260–350 nm with pyridine-centred π–π* absorptions at shorter wavelengths <300 nm. The lowest energy absorption band peaked at 547, 550 and 542 nm for L^1, L^2 and L^3 respectively, with corres-ponding molar absorptivities ca. 10^4 M^{-1} cm^{-1}. The lowest energy band can be assigned to an intramolecular charge transfer (ICT) dominated transition[20] that is anthraquinone-centred and derived from the amine-donor/quinone-acceptor chromophore (note that this is distinct from the quinone based n–π* which lies at much higher energy). This obser-vation is consistent with previous reports on amino-substi-tuted anthraquinone species.[21] The subtle variation in the wavelength of the absorption is likely to reflect the donating ability of the particular amine substituent, with stronger donors inducing a bathochromic shift in the ICT band.

Excitation of the ICT band for each of the ligands resulted in visible emission ca. 630 nm with a corresponding excitation peak at ca. 540 nm, which strongly correlates with the assigned ICT band in the absorption spectra. The resultant Stokes' shift (~2700 cm^{-1}) and short lifetime (τ ~ 1–2 ns) are consistent with a fluorescence from an ICT dominated excited state. Both absorption and emission data obtained in a range of solvents showed that these chromophores show classical positive solvatochromism (see ESI†), wherein polar solvents induce a bathochromic shift in the absorption/emission bands.

As expected the ligand-centred bands in each case domi-nated the absorption spectra of the complexes, where the lowest energy absorption was again attributed to the ICT band of the anthraquinone ligand. However, upon complexation of Ln(III), each spectrum revealed a subtle hypsochromic shift for this transition, suggesting a minor perturbation of the ICT state in the presence of the trivalent metal ion. Visible region luminescence studies on the Gd(III) complexes firstly revealed retention of the anthraquinone-based emission and secondly, a notable bathochromic shift (relative to the free ligands) of the ligand-based ICT fluorescence to ca. 664–679 nm; this latter observation provided key spectroscopic evidence for the stability of the complexes in solution.

In order to assess the potential of the these new anthra-quinone-based ligands as sensitising chromophores, additional low temperature measurements were obtained on solvent

glasses (ethanol/methanol 5 : 1) at 77 K for the Gd(III) com-plexes. It was noted that the peak position at 77 K was hypso-chromically shifted relative to the room temperature fluorescence peak. This shift is therefore attributed to the medium and temperature effects upon the ICT fluorescent state. It has been noted previously that amino-substituted anthraquinones, in contrast to halo-substituted variants,[22] do not generally show phosphorescence[23] with only limited evi-dence for a $^3n–\pi^*$ emissive state.[24]

For the near-IR Ln(III) complexes, the observed dual emis-sion characteristics in methanol solution were ascribed to two origins. Firstly, each of the complexes retained the ICT anthra-quinone-based fluorescence at ca. 670 nm; secondly, additional weaker bands in the near-IR region were observed, which are associated with the lanthanide-centred transitions and consistent with the inclusion of a Ln(III) ion. For the Ln-based emission these new chromophores facilitate long wave-length visible light sensitisation. This was best illustrated with L^3: for Yb-L^3 excitation at 535 nm yielded the characteristic structured Yb(III) emission at 950–1050 nm consistent with $^2F_{5/2} \rightarrow {}^2F_{7/2}$ (Fig. 4). Nd-L^3 revealed near-IR emission at 1058 nm ($^4F_{3/2} \rightarrow {}^4I_{11/2}$) with a much weaker feature at ca. 1340 nm, corresponding to $^4F_{3/2} \rightarrow {}^4I_{13/2}$; Er-$L^3$ gave a very weak broad emission feature centred around 1540 nm and assigned to the $^4I_{13/2} \rightarrow {}^4I_{15/2}$ transition. Near-IR steady state spectra obtained for the Ln(III) complexes of L^1 and L^2 only revealed extremely weak peaks, which were often superimposed or obscured by the tail of the anthraquinone-based ICT fluorescence (for example see Fig. S5, ESI†). However, it was possible to obtain supporting near-IR luminescence lifetime measurements (Table 1; see also further examples of fitted decay profiles in Fig. S5–S12, ESI†), providing decay profiles for each of the near-IR complexes. It is noteworthy that the lifetime values obtained in MeOH for the Nd(III) species are short. Non-radia-tive deactivation of Nd(III) is enhanced by C–H and N–H oscil-lators,[25] and it is clear from the modelling studies that these will be proximate to the Nd(III) centre. Although unlikely, given the supporting evidence from the analogous Yb(III) complexes, partial dissociation of the ligand in solution cannot be ruled out. Overall, time-resolved measurements on the complexes confirmed the long-lived nature of the Ln-based emission and also allowed a qualitative insight into the likely extent of sol-vation at the Ln(III) centre.

Using the values obtained in CH_3OH/CD_3OD allowed the approximation of q, the number of Yb(III)-bound solvent mole-cules (Table 1), calculated from $q = 2(k_{CH_3OH} - k_{CD_3OD} - 0.05)$ where k_H and k_D are the observed rate constants for the luminescence in μs^{-1}.[26] The calculations show that for the Yb(III) complexes, q reduced from ~4 (L^2) to ~2.5 (L^1) to ~1 (L^3). This suggests that for Yb-L^2 the coordination sphere is prob-ably six coordinate and likely to comprise the dipicolyl amine units with minimal contribution from the more remote anthraquinone core (Fig. 3); the latter is supported by the minimal perturbation of ligand-centred bands in the UV-vis spectra of the L^2 complexes. The data for Yb-L^1 is consistent with an intermediate situation where the Yb(III) is less solvated and the hypsochromically shifted anthraquinone absorption band of the complex possibly alludes to a coordinative contri-bution from the quinone unit (Fig. 5) as supported by the com-putational studies described earlier.

For Yb-L^3 the low q value and long lifetime in MeOH suggests a much more effective exclusion of solvent from the inner coordination sphere. This could be attributed to the coordinative participation of the oxygen donors of the two 1,3-diaminopropan-2-ol moieties, which can contribute to give a potential octadentate donor set for Yb(III) (Fig. 5). The compu-tational modelling studies support such an interaction. For the analogous parameters obtained from the Nd(III) species the general trend is the same with respect to the obtained q values (using $q = 290(k_{CH_3OH} - k_{CD_3OD}) - 0.4$) although they are gener-ally larger, as expected for the much larger ionic radius. It should also be noted that the associated errors of q values for non-aminocarboxylate type ligand architectures could be very significant.[27] Nonetheless, the increased inner sphere sol-vation for the Ln(III) complexes of L^1 and L^2 helps to explain

Table 1 Electronic spectroscopic data for the ligands and complexes

	Vis. absorption[a]	Vis. emission[b]	Near-IR τ/ns[c]	
Compound	λ_{abs}/nm	λ_{em}/nm	CH_3OH	CD_3OD
L^1	547	636	—	—
Nd-L^1	539	665	60	409
Gd-L^1	538	664	—	—
Er-L^1	540	664	—	448
Yb-L^1	539	663	699	5680
L^2	550	632	—	—
Nd-L^2	545	679	48	378
Gd-L^2	546	679	—	—
Er-L^2	548	678	—	597
Yb-L^2	543	675	441	6350
L^3	542	633	—	—
Nd-L^3	532	673	65	415
Gd-L^3	535	672	—	—
Er-L^3	535	671	—	567
Yb-L^3	534	671	1300	5360

[a] In MeOH. [b] In aerated MeOH, λ_{ex} = 535 nm. [c] λ_{ex} = 355 nm.

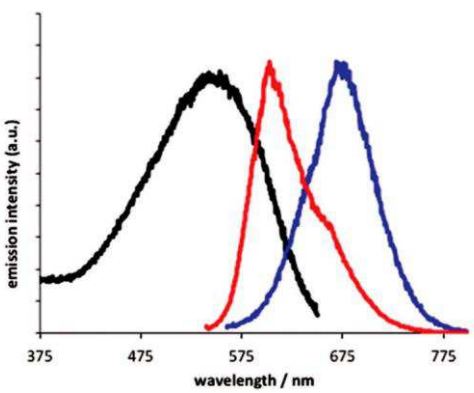

Fig. 3 Excitation (black), room temperature (blue) and low temperature (red) emission spectra for $[Gd(L^2)](OTf)_3$.

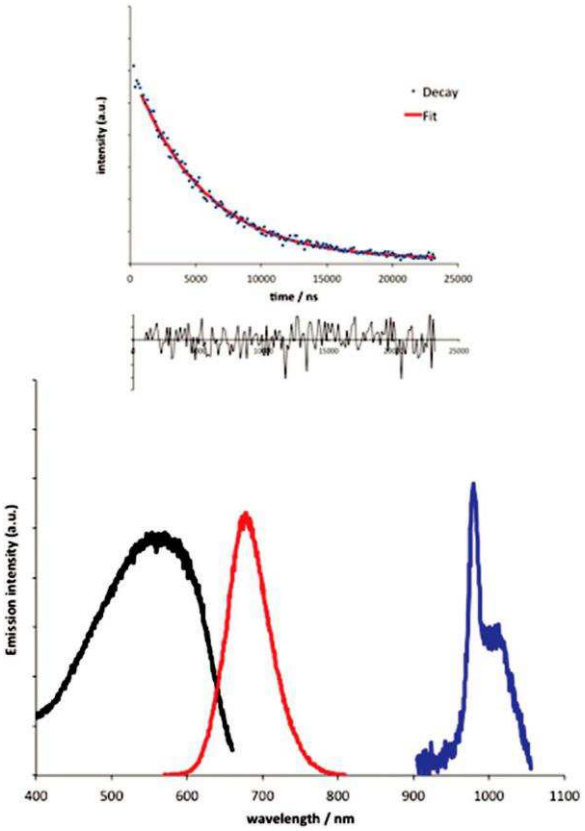

Fig. 4 Top: fitted decay profile for Yb-L^3 complexes (CD_3OD, λ_{em} = 980 nm, λ_{ex} = 355 nm). Bottom: excitation (black; λ_{em} = 975 nm), anthraquinone-centred (red) and ytterbium-centred (blue) emission for Yb-L^3 (CD_3OD, λ_{ex} = 525 nm).

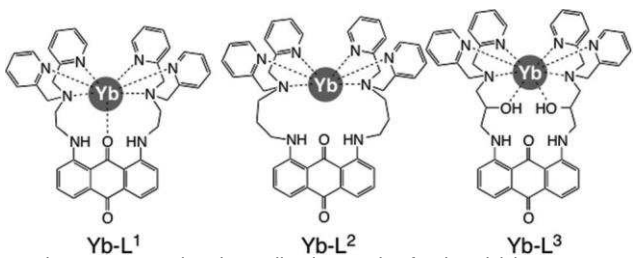

Fig. 5 Postulated coordination modes for the Yb(III) complexes.

the relative weakness of the observed near-IR emission bands of those species and the shorter lifetimes in methanol.

Experimental section

All reactions were performed with the use of vacuum line and Schlenk techniques. Reagents were commercial grade and used without further purification. ^1H and ^{13}C-{^1H} NMR spectra were recorded on an NMR-FT Bruker 400 or 250 MHz and ^{31}P-{^1H} NMR spectra on a Joel Eclipse 300 MHz spectro-meter and recorded in $CDCl_3$ or MeOD solutions. ^1H and ^{13}C-{^1H} NMR chemical shifts (δ) were determined relative to internal tetramethylsilane, $Si(CH_3)_4$ and are given in ppm. Low-resolution mass spectra were obtained by the staff at Cardiff University. High-resolution mass spectra were carried out at the EPSRC National Mass Spectrometry Facility at Swansea University, UK. Elemental analyses provided by London Metropolitan University. UV-Vis studies were performed on a Jasco V-650 spectrophotometer fitted with a Jasco temperature control unit in MeCN or MeOH solutions (10^{-5} M) at 20 °C. Photophysical data were obtained on a Jobin-Yvon–Horiba Fluorolog spectrometer fitted with a JY TBX picoseconds photodetection module in MeCN, MeOH or H_2O solutions. Emission spectra were uncorrected and excitation spectra were instrument corrected. The pulsed source was a Nano-LED configured for 372 or 459 nm output operating at 500 kHz. Luminescence lifetime profiles were obtained using the JobinYvon–Horiba FluoroHub single photon counting module and the data fits yielded the lifetime values using the provided DAS6 deconvolution software.

Scalar relativistic DFT calculations were carried out using the Gaussian 09 package,[28] with relativistic effects incorporated via the use of appropriate effective core potentials (ECPs). Geometry optimisations were performed at the M06 level,[29] with a basis set consisting of the Stuttgard-Dresden basis set plus ECP on Y and La, and cc-PVDZ on all remaining atoms.[30,31] The D3 version of Grimmes dispersion correction was included for all calculations.[32] Geometry optimisations were performed without symmetry constraints; the nature of the resulting molecular structures (i.e. minimum vs. saddle point) were verified with analytical frequency calculations.

Synthesis

Synthesis of Pro-L^1. Ethylene diamine (4.5 mL, 18 mmol) was added to a stirring suspension of 1,8-dichloroanthra-quinone (0.5 g, 1.8 mmol) in DMSO (5 mL). The mixture was heated to 150 °C for 3 h under dinitrogen and, after rapid addition of cold water to the hot solution and continued stir-ring for 1 h, the crude product was collected by filtration. The residue was then purified by column chromatography (silica) and the product was eluted as a purple (third) band using DCM–EtOAc (9 : 1). The solvent was removed in vacuo, and the product re-precipitated from methanol/diethyl ether, filtered and dried (yield 0.79 g, 34%). ^1H NMR (250 MHz, $CDCl_3$): δ_H 9.68 (2H, t, $^3J_{HH}$ = 5.0 Hz), 7.50–7.36 (4H, m), 6.98 (2H, dd, J_{HH} = 8.3, 1.0 Hz), 3.35 (4H, q, $^3J_{HH}$ = 5.8 Hz), 3.00 (4H, t, $^3J_{HH}$ = 6.3 Hz) ppm. IR ν_{max} (solid): 3271 (NH), 1612 (CO), 1566 (CO) cm^{-1}.

Synthesis of L^1. Pro-L^1 (0.23 g, 0.71 mmol) and 2-pyridine carboxaldehyde (0.27 mL, 2.8 mmol) were added to a stirring solution of sodium trisacetoxyborohydride (0.9 g, 4.2 mmol) in 1,2-dichloroethane (3.5 mL). The suspension was stirred under dinitrogen for 48 h. The reaction mixture pH was neutralized with sat. aq. $NaHCO_3$ before the product was extracted with ethyl acetate. The solvent was removed in vacuo to yield a dark purple solid (yield 0.41 g, 83%). ^1H NMR (400 MHz, $CDCl_3$): δ_H 9.75 (2H, t, $^3J_{HH}$ = 5.1 Hz), 8.41 (4H, d, $^3J_{HH}$ = 4.8 Hz),

7.56–7.30 (12H, m), 6.95–7.04 (4H, m), 6.85 (2H, dd, J_{HH} = 8.5, 0.9 Hz), 3.85 (8H, s), 3.41 (4H, q, $^3J_{HH}$ = 6.3 Hz), 2.87 (4H, t, $^3J_{HH}$ = 6.5 Hz) ppm. $^{13}C\{^1H\}$ NMR (75.6 MHz, $CDCl_3$): δ_C 40.8, 52.8, 60.6, 114.5, 115.1, 117.9, 122.0, 122.2, 123.1, 134.2, 136.5, 149.0, 151.0, 159.2, 184.6, 189.4 ppm. HRMS (ES) found m/z = 689.3344; calculated 689.3347 for $[C_{40}H_{41}N_8O_2]$. IR ν_{max} (MeCN): 3288 (NH), 1612 (CO), 1589 (CO) cm^{-1}. UV-vis (ε/M^{-1} cm^{-1}) (MeCN) λ_{max}: 260 (17 600), 304 (4500), 550 (7000) nm.

Synthesis of Pro-L^2. 1,3-Diaminopropane (1.5 mL, 18 mmol) was added to a stirring suspension of 1,8-dichloroanthra-quinone (0.5 g, 1.8 mmol) in DMSO (4.5 mL). The mixture was heated to 150 °C for 4 h. Cold water was added and the crude mixture was stirred for 1 h before the product was collected by filtration. The precipitate was re-dissolved in methanol before being precipitated with ether and collected by filtration to afford a dark purple solid (yield = 0.15 g, 23%). ^1H NMR (400 MHz, $CDCl_3$): δ H 7.46–7.44 (2H, m), 7.38–7.34 (m, 2H), 7.01–6.97 (m, 2H), 3.23 (4H, q, $^3J_{HH}$ = 5.2 Hz), 2.64 (4H, t,

$^3J_{HH}$ = 6.8 Hz), 2.01–1.89 (4H, m) ppm. IR ν_{max} (solid): 3275 (NH), 1612 (CO), 1591 (CO) cm^{-1}.

Synthesis of L^2. Pro-L^2 (0.15 g, 0.43 mmol), and 2-pyridine carboxaldehyde (0.16 mL, 1.67 mmol) were added to a stirring solution of sodium trisacetoxyborohydride (0.54 g, 2.56 mmol) in dichloroethane (1.5 mL). The suspenson was stirred under dinitrogen for 48 h. The reaction mixture pH was neutralized with sat. aq. $NaHCO_3$ before the product was extracted with ethyl acetate. The solvent was removed under reduced pressure to yield a dark purple oil (yield = 0.15 g, 48%). ^1H NMR (250 MHz, $CDCl_3$): δ_H 9.32 (2H, t, $^3J_{HH}$ = 5.2 Hz), 8.40 (4H, d, $^3J_{HH}$ = 4.8 Hz), 7.50–7.31 (12H, m), 7.05–6.92 (4H, m), 6.88 (2H, d, $^3J_{HH}$ = 8.4 Hz), 3.76 (8H, s, $^3J_{HH}$ = 14.4 Hz, CH_2), 3.22 (4H, q, $^3J_{HH}$ = 6.7 Hz), 2.67 (4H, t, $^3J_{HH}$ = 6.8), 1.90 (4H, app. quin., $^3J_{HH}$ = 6.9 Hz) ppm. $^{13}C\{^1H\}$ NMR (75.6 MHz, $CDCl_3$): δ_C 26.74, 40.82, 43.52, 51.52, 114.31, 114.78, 117.68, 122.03, 123.01, 134.09, 134.28, 136.46, 136.72, 148.89, 151.04, 159.52,
184.72, 188.62 ppm. HRMS (ES) found m/z = 717.3659; calcu-lated 717.3660 for $[C_{44}H_{45}N_8O_2]^+$. IR ν_{max} (MeCN): 3279 (NH),
1612 (CO), 1589 (CO) cm^{-1}. UV-vis (ε/M^{-1} cm^{-1}) (MeCN) λ_{max}: 238 (38 900), 325 (5800) (sh), 547 (9400) nm.

Synthesis of Pro-L^3. 1,3-Diamino-2-propanol (1.63 g, 0.018 mol) was added to a stirring suspension of 1,8-dichloro-anthraquinone (0.5 g, 1.8 mmol) in DMSO (4.5 mL). The mixture was heated to 150 °C for 4 h. Cold water was quickly added and the resultant crude product was stirred for 1 h before being collected by filtration. The product was re-precipi-tated from methanol/diethyl ether, before being collected by filtration and dried to afford a dark purple solid (yield 0.54 g, 78%). ^1H NMR (250 MHz, d_6-DMSO): δ_H 9.72 (2H, t, $^3J_{HH}$ = 5.1 Hz), 7.56 (2H, dd, J_{HH} = 8.0, 1.1 Hz), 7.37 (2H, d, $^3J_{HH}$ =
7.1 Hz), 7.25 (2H, d, $^3J_{HH}$ = 8.5 Hz), 3.68 (2H, br), 3.54–3.40 (4H, m), 3.26–3.18 (4H, m) ppm. IR ν_{max} (solid): 3262 (NH), –

Synthesis of L^3. Pro-L^3 (0.35 g, 0.91 mmol) and 2-pyridine carboxaldehyde (0.35 mL, 3.66 mmol) were added to a stirring solution of sodium trisacetoxyborohydride (1.15 g, 5.45 mmol) in 1,2-dichloroethane (3.5 mL). The reaction mixture was stirred under dinitrogen for 48 h. The reaction mixture pH was neutralized with sat. aq. $NaHCO_3$ before the product was extracted with ethyl acetate. The solvent was then removed under reduced pressure to yield a dark purple oil, which solidi-fied upon standing (yield 460 mg, 67%). ^1H NMR (400 MHz, $CDCl_3$): δ_H 9.32 (2H, br s), 8.40 (4H, d, $^3J_{HH}$ = 4.6 Hz), 7.50–7.31 (12H, m), 7.05–6.93 (4H, m), 6.88 (2H, dd, J_{HH} = 8.3, 2.7 Hz), 4.11–4.01 (4H, m), 3.76 (8H, s), 3.22 (4H, br), 2.87–2.70 (2H, m) ppm. $^{13}C\{^1H\}$ NMR (75.6 MHz, $CDCl_3$): δ_C 43.58, 46.97, 59.17, 67.81 114.55, 114.89, 117.88, 122.25, 123.25, 134.00, 134.26, 136.52, 136.74, 148.96, 151.21, 159.01,
184.68, 188.62 ppm. HRMS (ES) found m/z = 749.3570; calcu-lated 749.3558 for $[C_{44}H_{44}N_8O_4]^+$. IR ν_{max} (solid): 3281 (NH),
1615 (CO), 1570 (CO) cm^{-1}. UV-vis (ε/M^{-1} cm^{-1}) (MeCN) λ_{max}: 237 (60 100), 313 (10 300) (sh), 542 (12 900) nm.

Synthesis of $[Gd(L^1)](OTf)_3$. L^1 (105 mg, 0.147 mmol) and $Gd(OTf)_3$ (89 mg, 0.147 mmol) were dissolved in methanol and heated to reflux overnight. The reaction mixture was dried in vacuo and re-dissolved in minimum volume of acetonitrile before being precipitated with cold diethyl ether yielding a dark purple solid (yield 177 mg, 91%). MALDI MS (LD+) found m/z = 1022.1 calculated 1022.2 for $[M - 2OTf - H]^+$. Selected IR ν_{max} (solid): 3294 (NH), 1614 (CO), 1570 (CO), 1263 (OTf), 1215 (OTf), 1026 (OTf) cm^{-1}. UV-vis (ε/M^{-1} cm^{-1}) (MeCN) λ_{max}: 238 (55 000), 268 (52 200), 546 (12 300) nm.

Synthesis of $[Yb(L^1)](OTf)_3$. As for $[Gd(L^1)](OTf)_3$ but using L^1 (81 mg, 0.113 mmol) and $Yb(OTf)_3$ (72 mg, 0.113 mmol) (yield 118 mg, 78%). MALDI MS (LD+) found m/z = 1038.4; calculated 1038.2 for $[M - 2OTf - H]^+$. Selected IR ν_{max} (solid): 3295 (NH), 1614 (CO), 1568 (CO), 1225 (OTf), 1028 (OTf) cm^{-1}. UV-vis (ε/M^{-1} cm^{-1}) (MeCN) λ_{max}: 236 (35 900), 543 (7500) nm.

Synthesis of $[Nd(L^1)](OTf)_3$. As for $[Gd(L^1)](OTf)_3$ but using L^1 (68 mg, 0.095 mmol) and $Nd(OTf)_3$ (66 mg, 0.095 mmol) (yield 104 mg, 84%). MALDI MS (LD+) found m/z = 1008.6; calculated 1008.2 for $[M - 2OTf - H]^+$. Selected IR ν_{max} (solid): 3295 (NH), 1612 (CO), 1570 (CO), 1275 (OTf), 1227 (OTf), 1032 (OTf) cm^{-1}. UV-vis (ε/M^{-1} cm^{-1}) (MeCN) λ_{max}: 236 (37 800), 545 (8200) nm.

Synthesis of $[Er(L^1)](OTf)_3$. As for $[Gd(L^1)](OTf)_3$ but using L^1 (60 mg, 0.084 mmol) and $Er(OTf)_3$ (52 mg, 0.084 mmol) (yield 97 mg, 87%). MALDI MS (LD+) found m/z = 1032.3; cal-culated 1032.2 for $[M - 2OTf - H]^+$. Selected IR ν_{max} (solid): 3298 (NH), 1612 (CO), 1568 (CO), 1225 (OTf), 1029 (OTf) cm^{-1}. UV-vis (ε/M^{-1} cm^{-1}) (MeCN) λ_{max}: 238 (42 500), 272 (54 700), 548 (8000) nm.

Synthesis of $[Gd(L^2)](OTf)_3$. L^2 (50 mg, 0.073 mmol) and $Gd(OTf)_3$ (44 mg, 0.073 mmol) were dissolved in methanol and heated to reflux overnight. The reaction mixture was dried in vacuo and re-dissolved in minimum volume of acetonitrile before being precipitated with diethyl ether yielding a dark purple solid (yield 81 mg, 86%). MALDI MS (LD+) found m/z = 879.1; calculated 878.3 for $[M - 3OTf + 2H_2O]^+$. Selected IR ν_{max} (solid): 3290 (NH), 1615 (CO), 1573 (CO), 1271 (OTf), 1225 (OTf), 1032 (OTf) cm^{-1}. UV-vis (ε/M^{-1} cm^{-1}) (MeCN) λ_{max}: 259 (29 900), 314 (5600), 538 (9800) nm.

Synthesis of [Yb(L^2)](OTf)$_3$. As for [Gd(L^2)](OTf)$_3$ but using Yb(OTf)$_3$ (47 mg, 0.074 mmol) (yield 40 mg, 42%). MALDI MS (LD+) found m/z = 893.1; calculated 893.3 for $[M - 3OTf - 2H + 2H_2O]^+$. Selected IR ν_{max} (solid): 3291 (NH), 1618 (CO), 1570 (CO), 1270 (OTf), 1225 (OTf), 1032 (OTf) cm^{-1}. UV-vis (ε/M^{-1} cm^{-1}) (MeCN) λ_{max}: 258 (27 100), 315 (5500), 539 (10 100) nm.

Synthesis of [Nd(L^2)](OTf)$_3$. As for [Gd(L^2)](OTf)$_3$ but using Nd(OTf)$_3$ (51 mg, 0.073 mmol) (yield 74 mg, 80%). MALDI MS (LD+) found m/z = 864.0; calculated 864.2 for $[M - 3OTf - 2H + 2H_2O]^+$. Selected IR ν_{max} (solid): 1615 (CO) 1273 (OTf), 1225 (OTf), 1032 (OTf) cm^{-1}. UV-vis (ε/M^{-1} cm^{-1}) (MeCN) λ_{max}: 259 (42 000), 315 (7700), 539 (13 400) nm. Elemental analysis calculated for $C_{45}H_{40}N_8O_{11}F_9S_3Nd$: C, 42.22; H, 3.15; N, 8.75%; found C, 42.13; H, 3.09; N, 8.81%.

Synthesis of [Er(L^2)](OTf)$_3$. As for [Gd(L^2)](OTf)$_3$ but using Er(OTf)$_3$ (45 mg, 0.073 mmol) (yield 62 mg, 65%). MALDI MS (LD+) found m/z = 889.1; calculated 889.3 for $[M - 3OTf - 2H + 2H_2O]^+$. Selected IR ν_{max} (solid): 3294 (NH), 1615 (CO), 1573 (CO), 1270 (OTf), 1225 (OTf), 1031 (OTf) cm^{-1}. UV-vis (ε/M^{-1} cm^{-1}) (MeCN) λ_{max}: 258 (30 000), 312 (6000), 540 (10 700) nm. Elemental analysis calculated for $C_{45}H_{40}N_8O_{11}F_9S_3Er$: C, 41.47; H, 3.09; N, 8.60%; found C, 41.38; H, 3.03; N, 8.59%.

Synthesis of [Gd(L^3)](OTf)$_3$. L^3 (53 mg, 0.071 mmol) and Gd(OTf)$_3$ (43 mg, 0.071 mmol) were dissolved in methanol and refluxed overnight. The reaction mixture was dried in vacuo and re-dissolved in acetonitrile before being precipitated with diethyl ether yielding a dark purple solid (yield 55 mg, 62%). MALDI MS (LD+) found m/z = 900.202; calculated 900.254 for $[M - 3OTf - 2H]^+$. Selected IR ν_{max} (solid): 3400 br (NH and OH), 1616 (CO), 1571 (CO), 1271 (OTf), 1224 (OTf), 1032 (OTf) cm^{-1}. UV-vis (ε/M^{-1} cm^{-1}) (MeCN) λ_{max}: 258 (34 400), 304 (9000), 535 (15 700) nm.

Synthesis of [Yb(L^3)](OTf)$_3$. As for [Gd(L^3)](OTf)$_3$ but using Yb(OTf)$_3$ (47 mg, 0.074 mmol) (yield 34 mg, 34%). MALDI MS (LD+) found m/z = 916.125; calculated 916.268 for $[M - 3OTf - 2H]^+$. Selected IR ν_{max} (solid): 3368 br (NH and OH), 1615 (CO), 1572 (CO), 1271 (OTf), 1224 (OTf), 1031 (OTf) cm^{-1}. UV-vis (ε/M^{-1} cm^{-1}) (MeCN) λ_{max}: 258 (20 900), 311 (4800), 534 (9000) nm.

Synthesis of [Nd(L^3)](OTf)$_3$. As for [Gd(L^3)](OTf)$_3$ but using L^3 (59 mg, 0.079 mmol) and Nd(OTf)$_3$ (55 mg, 0.079 mmol) (yield 83 mg, 79%). MALDI MS (LD+) found m/z = 888.181; calculated 888.241 for $[M - 3OTf - 2H]^+$. Selected IR ν_{max} (solid): 3457 br (NH and OH), 1616 (CO), 1570 (CO), 1271 (OTf), 1224 (OTf), 1031 (OTf) cm^{-1}. UV-vis (ε/M^{-1} cm^{-1}) (MeCN) λ_{max}: 257 (30 300), 302 (8100), 532 (13 400) nm. Elemental analysis calculated for $C_{47}H_{44}N_8O_{13}F_9S_3Nd$: C, 42.12; H, 3.31; N, 8.36%; found C, 42.03; H, 3.34; N, 8.25%.

Synthesis of [Er(L^3)](OTf)$_3$. As for [Gd(L^3)](OTf)$_3$ but using L^3 (60 mg, 0.080 mmol) and Er(OTf)$_3$ (49 mg, 0.080 mmol) (yield 90 mg, 82%). MALDI MS (LD+) found m/z = 914.4; calcu-lated 914.3 for $[M - 3OTf]^+$. Selected IR ν_{max} (solid): 3410 br (NH and OH), 1616 (CO), 1570 (CO), 1270 (OTf), 1223 (OTf), 1032 (OTf) cm^{-1}. UV-vis (ε/M^{-1} cm^{-1}) (MeCN) λ_{max}: 258 (16 900), 303 (4300), 535 (7600) nm. Elemental analysis calculated for $C_{47}H_{44}N_8O_{13}F_9S_3Er$: C, 41.41; H, 3.25; N, 8.22%; found C, 41.38; H, 3.34; N, 8.19%.

Conclusions

In summary, we have presented the synthesis and characteris-ation of three new 1,8-disubstituted anthraquinone derived ligands that can bind trivalent lanthanide ions. The optical characteristics of the ligands provide effective visible light absorption and emission character via ICT excited states. The chromophores facilitate visible light sensitization of the Ln-based near-IR emission with the relative intensities of the emission bands dictated by the extent of inner sphere solvent exclusion from the Ln(III) centre.

Computational modelling studies on the three different ligands with either Y(III) or La(III) showed that these complexes are likely to exist as 1 : 1 species rather than 2 : 2 formulations. The calculations show that the latter is >1000 kJ mol^{-1} less favourable. In the absence of solid state structural information, the use of time-resolved luminescence measurements to probe the coordination sphere of the lanthanide ions allows a quali-tative insight into ligand binding modes. In this context, L^3, based upon the 1,3-diamino-2-propanol linking framework, provides a potentially octadentate donor set for the metal ion and leads to quite effective encapsulation of Yb(III) and shield-ing from solvent molecules as evidenced by the luminescence lifetimes. Such a binding mode was also supported by the computational modelling work. Further work will investigate the enhancement and optimisation of these ligand frame-works towards water-soluble variants; such systems should be amenable as prospective bimodal (optical/MR) imaging agents.[33]

Acknowledgements

We thank Cardiff University for support and the staff of the EPSRC Mass Spectrometry National Facility (Swansea University) for providing MS data.

Notes and references

1 E. E. Langdon-Jones and S. J. A. Pope, Coord. Chem. Rev., 2014, 269, 32.

2 H.-S. Bien, J. Stawitz and K. Wunderlich, in Anthraquinone Dyes and Intermediates, Ullmann's Encyclopedia of Indus-trial Chemistry, Wiley-VCH, 2000.

3 For example: M. Locatelli, Curr. Drug Targets, 2011, 12, 366; A. P. Krapcho, M. J. Maresch, M. P. Hacker, L. Hazelhurst, E. Menta, A. Olivia, S. Spinelli, G. Beggiolin, F. C. Giuliani, G. Pezzoni and S. Tognella, Curr. Med. Chem., 1995, 2, 803; Q. Liu, S. B. Kim, J. H. Ahn, B. Y. Hwang, S. Y. Kim and M. K. Lee, Nat. Prod. Res., 2012, 26, 1750; A. Baghiani, N. Charef, M. Djarmouni, H. A. Saadeh, L. Arrar and M. S. Mubarak, Med. Chem., 2011, 7, 639.

4 A. N. Diaz, J. Photochem. Photobiol., A, 1990, 53, 141.
5 Z. Yoshida and F. Takabayashi, Tetrahedron, 1968, 24, 933.

6 M. S. Khan and Z. H. Khan, Spectrochim. Acta, Part A, 2003, 59, 1409.
7 J. E. Jones, B. M. Kariuki, B. D. Ward and S. J. A. Pope, Dalton Trans., 2011, 40, 3498.
8 T. Moriuchi, T. Watanabe, I. Ikeda, A. Ogawa and T. Hirao, Eur. J. Inorg. Chem., 2001, 277.
9 For example: K. Mariappan, P. N. Basa, V. Balasubramanian, S. Fuoss and A. G. Sykes, Polyhedron, 2013, 55, 144.
10 N. Kaur and S. Kumar, Chem. Commun., 2007, 3069; E. Ranyuk, A. Uglov, M. Meyer, A. B. Lemeune, F. Denat, A. Averin, I. Beletskaya and R. Guilard, Dalton Trans., 2011, 40, 10491.
11 D. A. Gustowski, M. Delgado, V. J. Gatto, L. Echegoyen and G. W. Gokel, Tetrahedron Lett., 1986, 27, 3487; D. A. Gustowski, M. Delgado, V. J. Gatto, L. Echegoyen and G. W. Gokel, J. Am. Chem. Soc., 1986, 108, 7553; L. Echegoyen, D. A. Gustowski, V. J. Gatto and G. W. Gokel, J. Chem. Soc., Chem. Commun., 1986, 220; M. Delgado, D. A. Gustowski, H. K. Yoo, V. J. Gatto, G. W. Gokel and L. Echegoyen, J. Am. Chem. Soc., 1988, 110, 119; Z. Chen, O. F. Schall, M. Alcala, G. W. Gokel and L. Echegoyen, J. Am. Chem. Soc., 1992, 114, 444; P. N. Basa, A. Bhowmick, M. M. Schulz and A. G. Sykes, J. Org. Chem., 2011, 76, 7866.

12 K. Mariappan, M. Alaparthi, M. Hoffman, M. A. Rama, V. Balasubramaniam, D. M. John and A. G. Sykes, Dalton Trans., 2015, 44, 11774.
13 R. G. Balasingham, C. F. Williams, H. J. Mottram, M. P. Coogan and S. J. A. Pope, Organometallics, 2012, 31, 5835.

14 M. Utsuno, T. Yutaka, M. Murata, M. Kurihara, N. Tamai and H. Nishihara, Inorg. Chem., 2007, 46, 11291.
15 J. E. Jones and S. J. A. Pope, Dalton Trans., 2009, 8421.
16 J. E. Jones, A. J. Amoroso, I. M. Dorin, G. Parigi, B. D. Ward, N. J. Buurma and S. J. A. Pope, Chem. Commun., 2011, 47, 3374.
17 See comment within: A. Beeby, B. P. Burton-Pye, S. Faulkner, G. R. Motson, J. C. Jeffrey, J. A. McCleverty and M. D. Ward, Dalton Trans., 2002, 1923.
18 L. S. Natrajan, P. L. Timmins, M. Lunn and S. L. Heath, Inorg. Chem., 2007, 46, 10877.
19 B. Cordero, V. Gómez, A. E. Platero-Prats, M. Revés, J. Echeverría, E. Cremades, F. Barragán and S. Alvarez, Dalton Trans., 2008, 2832.
20 E. A. Perpete, V. Wathelet, J. Preat, C. Lambert and D. Jacquemin, J. Chem. Theory Comput., 2006, 2, 434.
21 A. N. Diaz, J. Photochem. Photobiol., A, 1990, 53, 141.
22 K. Hamanoue, Y. Kajiwara, T. Miyake, T. Nakayama, S. Hirase and H. Teranishi, Chem. Phys. Lett., 1983, 94, 276.
23 N. S. Allen, J. F. McKellar, B. M. Moghaddam and G. O. Phillips, J. Photochem., 1979, 11, 101; N. S. Allen, B. Harwood and J. F. McKellar, J. Photochem., 1978, 9, 559.
24 N. S. Allen, B. Harwood and J. F. McKellar, J. Photochem., 1978, 9, 565.
25 S. Faulkner, S. J. A. Pope and B. P. Burton-Pye, Appl. Spectrosc. Rev., 2005, 40, 1; C. Bischof, J. Wahsner, J. Scholten, S. Trosien and M. Seitz, J. Am. Chem. Soc., 2010, 132, 14334.
26 A. Beeby, I. M. Clarkson, R. S. Dickins, S. Faulkner, D. Parker, L. Royle, A. S. de Sousa, J. A. G. Williams and M. Woods, J. Chem. Soc., Perkin Trans. 2, 1999, 493.
27 S. Faulkner, A. Beeby, M. C. Carrie, A. Dadabhoy, A. M. Kenwright and P. G. Sammes, Inorg. Chem. Commun., 2001, 4, 187.
28 M. J. Frisch, G. W. Trucks, H. B. Schlegel, G. E. Scuseria, M. A. Robb, J. R. Cheeseman, G. Scalmani, V. Barone, B. Mennucci, G. A. Petersson, H. Nakatsuji, M. Caricato, X. Li, H. P. Hratchian, A. F. Izmaylov, J. Bloino, G. Zheng, J. L. Sonnenberg, M. Hada, M. Ehara, K. Toyota, R. Fukuda, J. Hasegawa, M. Ishida, T. Nakajima, Y. Honda, O. Kitao, H. Nakai, T. Vreven, J. A. Montgomery Jr., J. E. Peralta, F. Ogliaro, M. Bearpark, J. J. Heyd, E. Brothers, K. N. Kudin, V. N. Staroverov, T. Keith, R. Kobayashi, J. Normand, K. Raghavachari, A. Rendell, J. C. Burant, S. S. Iyengar, J. Tomasi, M. Cossi, N. Rega, J. M. Millam, M. Klene, J. E. Knox, J. B. Cross, V. Bakken, C. Adamo, J. Jaramillo, R. Gomperts, R. E. Stratmann, O. Yazyev, A. J. Austin, R. Cammi, C. Pomelli, J. W. Ochterski, R. L. Martin, K. Morokuma, V. G. Zakrzewski, G. A. Voth, P. Salvador, J. J. Dannenberg, S. Dapprich, A. D. Daniels, O. Farkas, J. B. Foresman, J. V. Ortiz, J. Cioslowski and D. J. Fox, Gaussian 09, Revision D.01, Gaussian Inc., Wallingford CT, 2013.

29 Y. Zhao and D. G. Truhlar, Theor. Chem. Acc., 2008, 120, 215.
30 D. Andrae, U. Haussermann, M. Dolg, H. Stoll and H. Preuss, Theor. Chim. Acta, 1990, 77, 123.
31 T. H. Dunning Jr., J. Chem. Phys., 1989, 90, 1007.
32 S. Grimme, J. Antony, S. Ehrlich and H. Krieg, J. Chem. Phys., 2010, 132, 154104.
33 A. J. Amoroso and S. J. A. Pope, Chem. Soc. Rev., 2015, 44, 4723.